Available online at www.sciencedirect.com

ScienceDirect

Procedia Engineering 144 (2016) 3 – 25

Procedia Engineering

www.elsevier.com/locate/procedia

12th International Conference on Vibration Problems, ICOVP 2015

Advances in Aero Structures

J S Rao[1]

Kumaraguru College of Technology, Coimbatore, Chief Science Officer (Consulting), Altair Engineering, Bangalore, India.

Abstract

With the advent of high performance computing the approximate engineering approach of 20th century has given way to Science to Engineering approach directly from 17th century to 21st century. The concept of simultaneous design and optimization that began with Science Revolution with Brachistochrone Problem has helped in achieving optimum designs from the concept particularly in complex aeronautical structures. This paper describes through some examples the way in which aircraft structural designs can be produced in a short period of time using SBES approach through HPC.
Concept design of an aircraft wing given the loads and the airfoil shape from CFD
Achieving a composite structure through optimization principles
Impact analysis from bird hits
Fluid Structure Interaction and flutter analysis
Engine-Wing integrated structure analysis attempts

Peer-review under responsibility of the organizing committee of ICOVP 2015

Keywords: Tuned mass damper, Piezoelectric actuator, Method of multiple scales, Fixed point theory.

1. Introduction

Geometry (Shape) played an important role in ancient civilizations and optimization problems had their roots in Greek science. Euclid (323-285 B.C.) is a great Greek mathematician best known for his treatise on geometry, which influenced the development of Western mathematics for over 2000 years, see Rao (1992). With modern design practices of globally elastic and locally plastic structures, it is once again the shape of mechanical components that is playing a significant role in optimizing weight, maximizing life etc.

In Euclid's book III of the Elements, see Heath (1956), the basic ideas of optimization are embedded; there is a discussion of the greatest and least straight lines that can be drawn from a point to the circumference of a circle. Also in book VI, it is discussed about the parallelogram of greatest area with a given parameter.

Archimedes (287-212 BC) of Syracuse in Sicily is believed by many to be the first mathematical genius the world has so far produced. He is also believed by many to put his accomplishments into written form, see Heath (1897) and Crombie (1979). In his work on division of a sphere in two parts so that the volume ratio of these parts is equal to a given ratio, Archimedes solves the problem of finding the maximum of $f(x)=x^2(x-a)$. Amongst the Alexandrian school of engineers is undoubtedly Hero who lived sometime during the second century BC. He proved that light travels between two points through the path with shortest length when reflecting from a mirror see Pederson (1993).

[1] Corresponding Author.
E-mail address: rao_js@yahoo.com

Peer-review under responsibility of the organizing committee of ICOVP 2015
doi:10.1016/j.proeng.2016.05.002

The event which most historians of science call the scientific revolution can be dated roughly as having begun in 1543, the year in which Nicolaus Copernicus published his *De revolutionibus orbium coelestium*, see Rao (2011). Scientific revolution made rapid strides beginning with Isaac Newton (1786) and Gottfried Leibniz (1684) that developed fundamentals of calculus and calculus of variations.

Euclid's influence is so profound that it is said that Newton in 1663, when he was just 20 years old, bought a book on astrology out of a curiosity to see what is there in it. When he could not understand an illustration in this book, he bought a book on Trigonometry, and to follow the geometry in this book in turn, he bought the book of Euclid's elements of geometry. Armed with these books, he discovered in 1665, the subject of differential calculus, while he was still an undergraduate student at Cambridge.

It is worth noting the way in which Calculus of Variations was invented by Newton. Johann Bernoulli challenged fellow mathematicians at that time to solve an unresolved issue called Brachistochrone problem, see Rickey (1996), specifying the curve connecting two points displaced from each other laterally, along which a body, acted upon only by gravity, would fall in the shortest time. From Greek, βράχιστος, *brachistos* means *the shortest*, χρόνος, *chronos* - *time* giving the name Brachistochrone. He set a dead line of six months originally and extended it to a year and a half at the request of another fellow mathematician. It is said that the challenge was delivered to Newton at 4.00 PM on January 29, 1697. Newton before leaving for work next morning invented calculus of variations to solve this problem. The subject of calculus of variations plays an important role in the theory of optimization and analysis that will be discussed in this paper.

2. Brachistochrone – The First Optimization Problem

The Brachistochrone problem is specifying the curve connecting two points displaced from each other laterally, along which a body, acted upon only by gravity, would fall in the shortest time. Newton showed that the required solution is a cycloid by discovering calculus of variations. Rao (2012) treated this as analysis problem or design problem. Exact solution using classical optimization and Galerkin solution with a one term approximation (analysis) are given in Fig. 1 along with a straight line path for a comparison. Table 1 gives the time taken on Cycloid

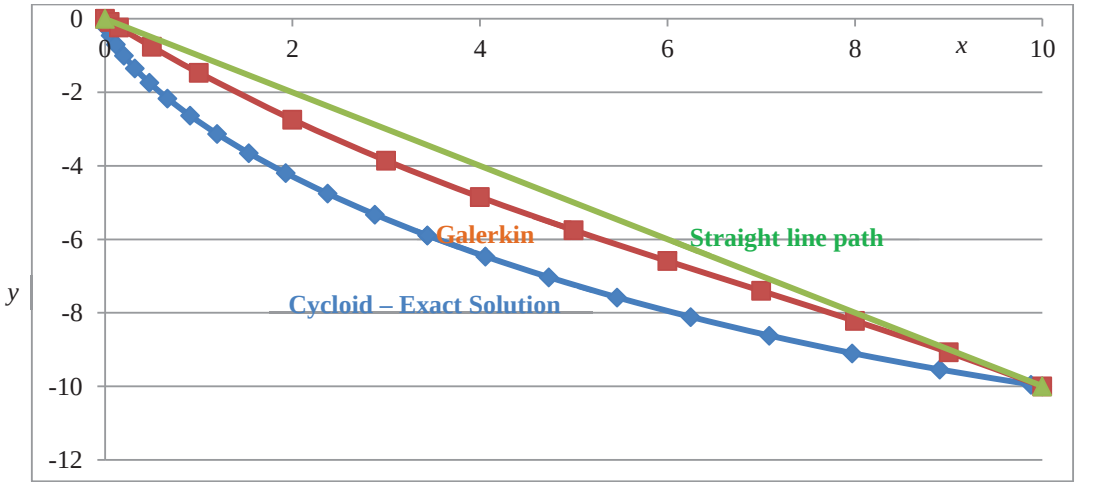

Fig. 1 Brachistocrone Solution

This time 1.512 sec is the least time for travel between points (1) and (2), considerably less than straight line path time 2.016 sec and slightly more than the vertical fall 1.426 sec.

We conclude from the above that the optimization problem posed by Johann Bernoulli is also analysis problem through Variational Calculus; the reason for bringing out this point is that all analysis methods essentially are approximate methods and today the design exercises for structures are carried out by using finite element methods which also are approximate methods from Calculus of Variations. Therefore the design and optimization procedures

belong to the same class. This principle is used to design an aircraft wing from first principles rather than traditional design procedures and then optimize for weight.

Table 1 Time taken on Cycloid Path

No.	*x*	*y*	*t*	*V*
1	0	0	0	0
2	0.118	-0.701	0.191	3.714
3	0.473	-1.738	0.187	5.848
4	0.908	-2.634	0.138	7.199
5	1.928	-4.197	0.205	9.087
6	4.058	-6.467	0.276	11.280
7	7.086	-8.622	0.285	13.025
8	10	-10	0.230	14.029
			1.512	

3. Simultaneous Design and Optimization

Conventional design procedures followed during the 20th century are essentially test based compared to the simulation based methods developed towards the end of 20th century. The simulation based designs have obvious advantages in cutting costs and saving time. With the advent of high speed computational era, many industries have shifted to these design methodologies.

The designers' interest in the beginning essentially lay in reducing the bulk weight of the mid-20th century designs which wasted power in propulsion. The original shape optimization interest of Archimedes time has returned now to machine parts rather than land. Though optimization or mathematical programming made deep strides in linear programming, nonlinear programming, geometric programming, genetic algorithms in thermal, structures, fluids … and economics areas, see Vanderplaats (1984), Pike (1992), Rao (1996), very little has been achieved till recently in the design of complex machine structural components.

The pioneering work of modern structural topology can be traced back to 1981 when Cheng and Olhoff, see Keng-Tuno (1981) introduced the concept of microstructure to structural optimization in studying the optimum thickness design of a solid elastic plate for minimum compliance. A continuum approach to structural topology optimization was first introduced by Bendsøe and Kikuchi (1988). Optimization of Finite Element-based structures is acknowledged as a useful methodology for achieving important improvements in product design and is widely used in automotive and aerospace industries.

Initially weight optimization was achieved from existing proven structures by identifying strain energy density locations of the structure which are low in density. Manually these locations are determined to readjust the material distribution and removing it wherever the load path can be dispensed off. This will be purely design based approach in identifying these areas and manually readjusting the locations where material can be removed and occasionally where the material is required to be added to strengthen the weak areas, see Rao (2003).

Because of heavy demand for the optimization in linear structures that are widely employed in various sectors of industry since World War II, the weight optimization was developed through maintaining the compliance of the structure in readjusted material distribution. The load path (shape of the structure where maximum load is borne) was determined, the dead weight is removed and the structure reshaped by sizing of suitable structural members. This came to be known as a new branch of optimization called topology or shape optimization. There are several codes being developed in recent years, the most promising are from Altair HyperWorks (2011). This suit of codes works as a platform to combine various disciplines of Physics together with Preprocessors and Postprocessors for data storage, display and math. One of them in this suit is dedicated to linear structures optimization called OptiStruct and another optimization solver called HyperStudy capable of handling linear, nonlinear, multiphysics and multi-constraint

problems. Detailed methodology for shape optimization of a typical machine turbomachine blade roots is presented using Altair OptiStruct and Altair HyperStudy tools by Rao and Suresh (2006) and multiphysics problems of flow and conjugate heat transfer by Rao, Saravanakumar and Kumar (2006). These are however in the category of optimization of designed problems.

NAL and ADA in the last decade were looking at a concept as well as optimized wing design in a short period of time and thus the first application of simultaneous design and optimization took place. The wing shape itself is derived from a CFD analysis and the design of the wing structure is to be made in a short time as possible.

Consider the design of an aircraft wing made of Aluminum with Wing Span 13.5 m, Constant chord wing span 4.74 m, and Tapered chord wing span 8.76 m as given in Fig.2. Chord length in Fig. 3 at wing root is 2.68 m and at wing tip 1.39 m. Young's Modulus = 70000 MPa, Poisson's ratio = 0.33 and Density = 2.60×10-09 tonne/mm3. The loads taken on the wing include flight load, fuel load and engine load. The pressure values at stations every 500 mm apart the wing span are given in Fig. 4. Fuel tank starts from 20% and ends at 85% of constant chord wing span. Center of Gravity of the fuel tank is at 1.27 m from leading edge and 2.5 m from wing root. Fuel load is 1730 Kg per wing. The engine is mounted from 85% to 98% of constant chord wing span; and its weight is 800 Kg. It is assumed to be mounted on front and rear spars through two ribs and the weight distribution at the four nodes of intersection between the two spars and ribs see Rao et al (2008). The wing was constrained in degrees of freedom analogous to a cantilever beam. All the nodes in the root tip face of the airfoil section were constrained.

As against the normal design procedure of developing a wing structure with ribs, spars and determining the sizes of various cross-sections and checking for their structural integrity and then possible optimization to decrease weight where possible, the design is conceptualized directly from optimization. Topology optimization suggested the structural load path as shown in Fig. 5. The structure is then divided into the three different regions for the ribs as shown in Fig. 6. Fig. 7 shows how the spars of the wing are identified that defines the shapes to be angular cross-sections. Fig. 8 likewise shows the front and middle ribs.

This procedure is continued and finally a size optimization is performed to determine the final structure as shown in Fig. 9.

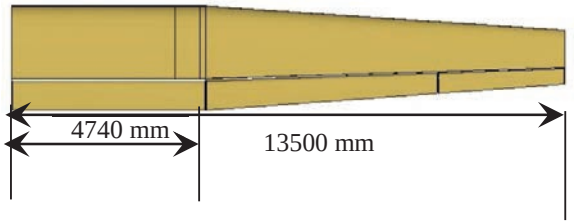

Fig. 2 Wing Planform

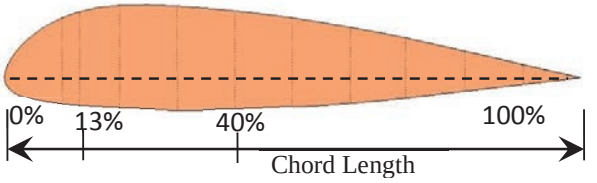

Fig. 3 Airfoil

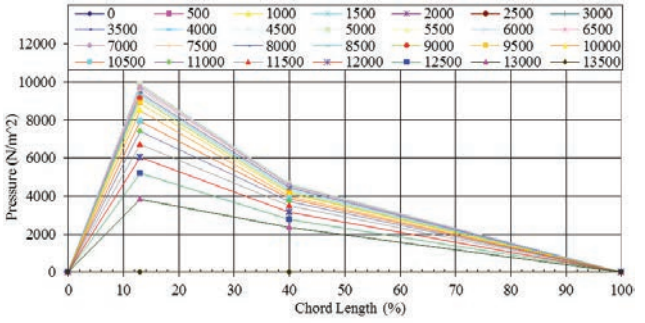

Fig. 4 Pressure Loads

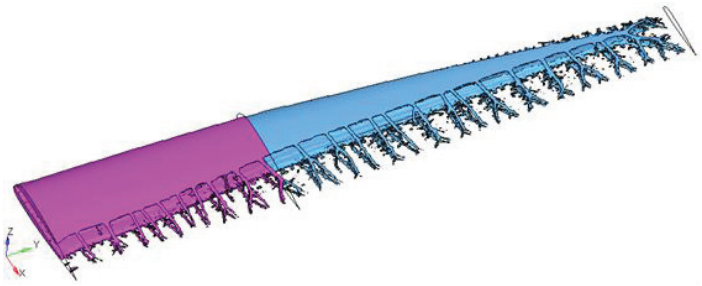

Fig. 5 Load Path of the Required Wing Structure

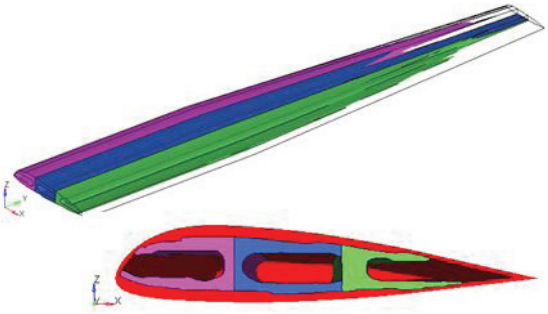

Fig. 6 Division into Front, Middle and Rear Rib Regions

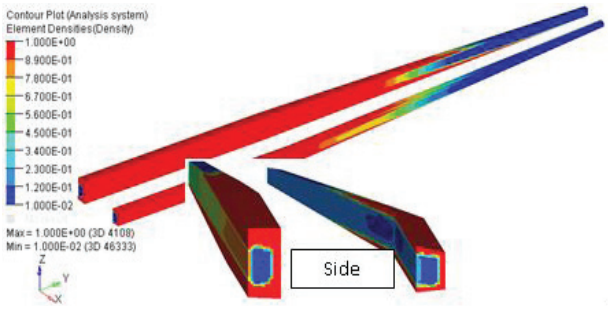

Fig. 7 Spar sections identified by topology optimization

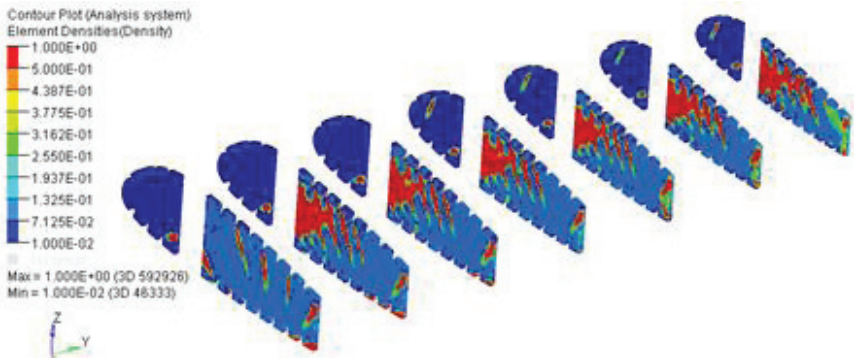

Fig. 8 Nose and Middle Ribs by topology optimization

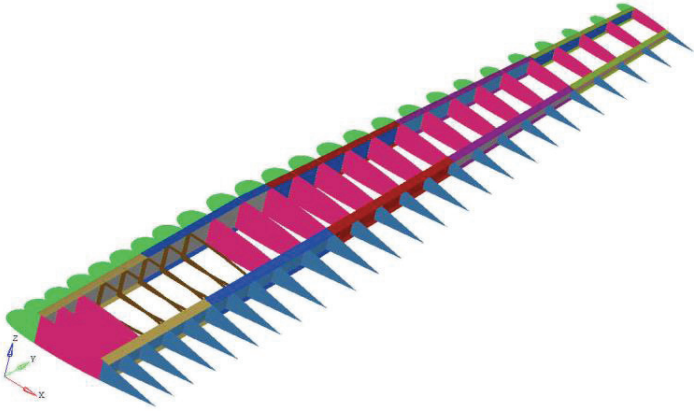

Fig. 9 Final Design obtained through combined analysis and optimization

4. Composite Structure from Topology Optimization

Similar approach is used by Rao and Kiran (2010) in converting the isotropic wing to a composite wing for further reduction in weight. Stress-Strain relations for different angle ply laminae are given by Rao (1998). Optimization for the composite structure is carried out in three phases:

Phase I - Concept: Free-Size or Topology Optimization

Composite free-sizing optimization is to create design concepts that utilize all the potentials of a composite structure where both structure and material can be designed simultaneously. By varying the thickness of each ply with a particular fiber orientation for every element, the total laminate thickness can change 'continuously' throughout the structure, and at the same time, the optimal composition of the composite laminate at every point (element) is achieved simultaneously. Manufacturing constraints like lower and upper bound thickness on the laminate, individual orientations and thickness balance between two given orientations can be defined.

Phase II – Detailed Design: Ply-Bundle Sizing with ply-based FEA modeling

Sizing optimization is performed to control the thickness of each ply bundle, while considering all design responses and optional manufacturing constraints. Ply thicknesses are directly selected as design variables. Composite plies are shuffled to determine the optimal stacking sequence for the given design optimization problem while also satisfying manufacturing constraints like control on number of successive plies of same orientation, pairing 45° and -45° orientations together etc.

Phase III – Detailed Design: Ply Stacking Sequence Optimization

Composite plies are shuffled to determine the optimal stacking sequence for the given design optimization problem while also satisfying additional manufacturing constraints like,

- The stacking sequence should not contain any section with more than a given number of successive plies of same orientation.
- The 45° and -45° orientations should be paired together
- The cover and/or core sections should follow a predefined stacking sequence

The model in Fig. 9 is now taken as baseline to develop the composite structure.

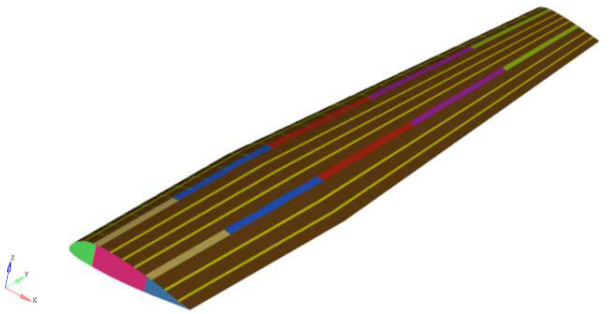

Fig. 10 Regions for Free Sizing

Phase 1: Free-Size or Topology Optimization: Free size optimization was performed to determine the thickness and laminate family within the chosen regions of the CAD model. The wing in Fig. 9 is divided in to regions for size optimization as shown in Fig. 10. Objective functions in this optimization are mass and compliance and minimization of the same. The design space is limited to ribs only in this exercise. The base laminate chosen is symmetric without a core with 10.16 mm thickness for all plies as given in Table 2. Carbon Fiber Reinforced Plastic is chosen for the laminate plies as given.

The results of free size optimization for the four plies in all the ribs are given in Fig. 11. We notice that the ribs near the wing root have higher material density or should be thicker and those nearer to the tip do not carry much load and therefore can be lighter.

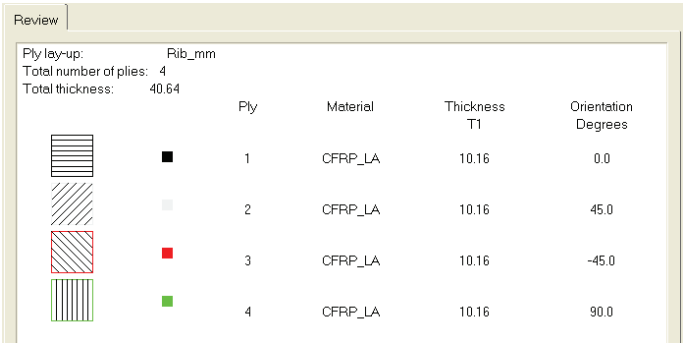

Table 2 Base Laminate

	Symbol	Units	Properties
E	E1	N/mm^2	1.52×10^5
E	E2	N/mm^2	9650
G	G12	N/mm^2	5930
n	NU12		0.321
r	Rho	Tonne/mm^3	1.53×10^{-9}

Phase 2: Ply-Bundle Sizing with Ply-Based FEA modeling: The size optimization of the Plies obtained in Phase 1 with Free Size or Topology optimization was next performed to determine the thickness and laminate family within all the Ribs, Skin and Spars. Objective functions are again mass and compliance and minimization of the same. The results obtained in all Ribs are given in Fig. 12.

A review of the design process up to now reveals that we established the optimum ply shape and patch locations in phase 1 (free size optimization) and subsequently optimized the ply bundle thicknesses in phase 2 (ply bundle sizing optimization), allowing us to determine the required number of plies. These ply bundles represent the Optimal Ply Shapes (Coverage Zones). Figure 13 shows the optimal ply shapes thickness contour of ply bundles of the 90º Super Ply.

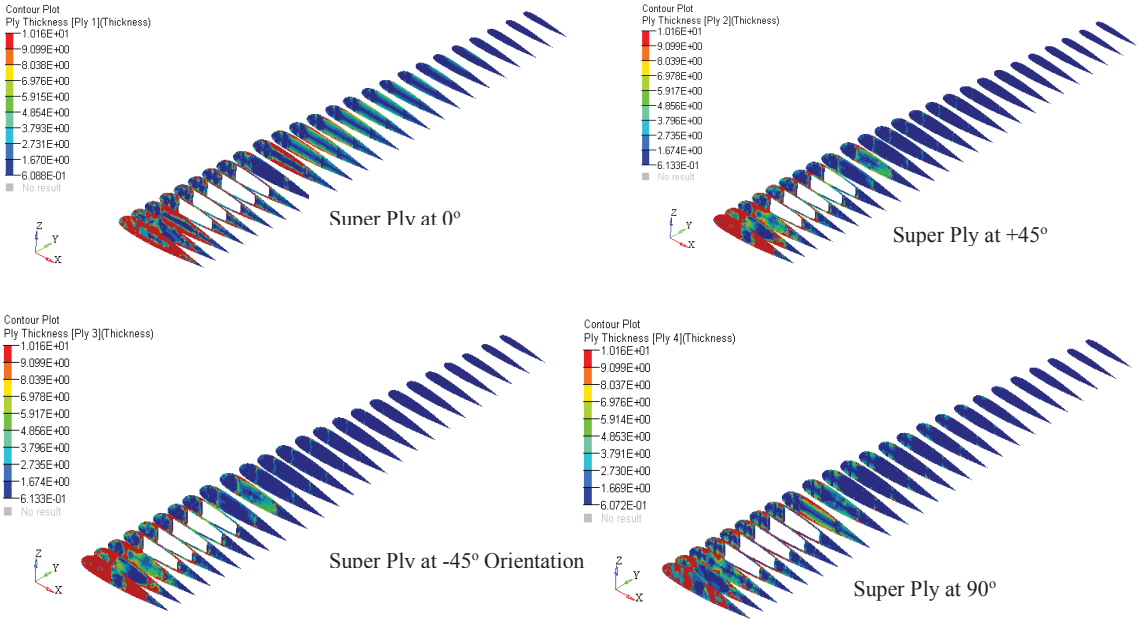

Fig. 11 Free Size Optimization for of all Ribs

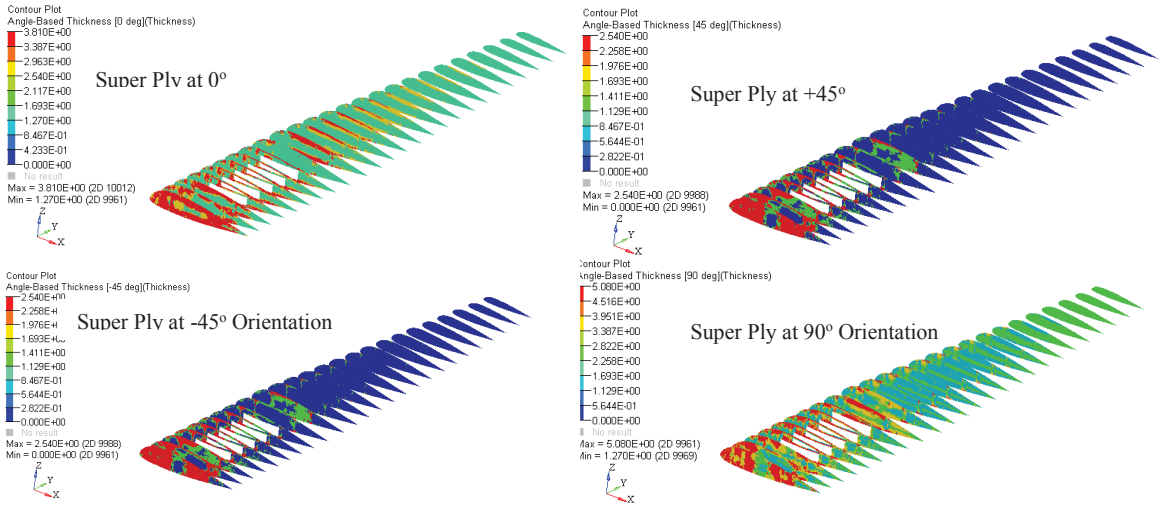

Fig. 12 Size Optimization f0r all Ribs

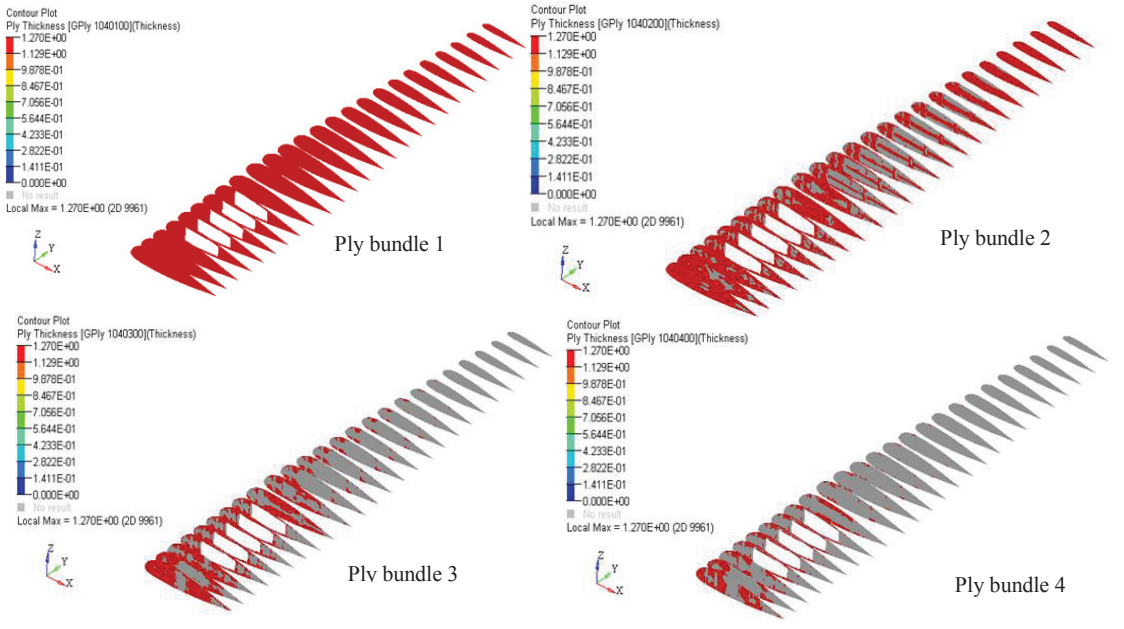

Fig. 13 Optimal Ply Shapes thickness contour of ply bundles of 90º Super Ply

Similarly the Optimal Ply Shapes thickness contours of ply bundles for the 0º +45º and -45º Super Plies are obtained (not given here).

After completing the ply bundle sizing optimization, the optimized thickness contour of all ply bundles are post processed. The total size optimization of the ribs is shown in Fig 14.

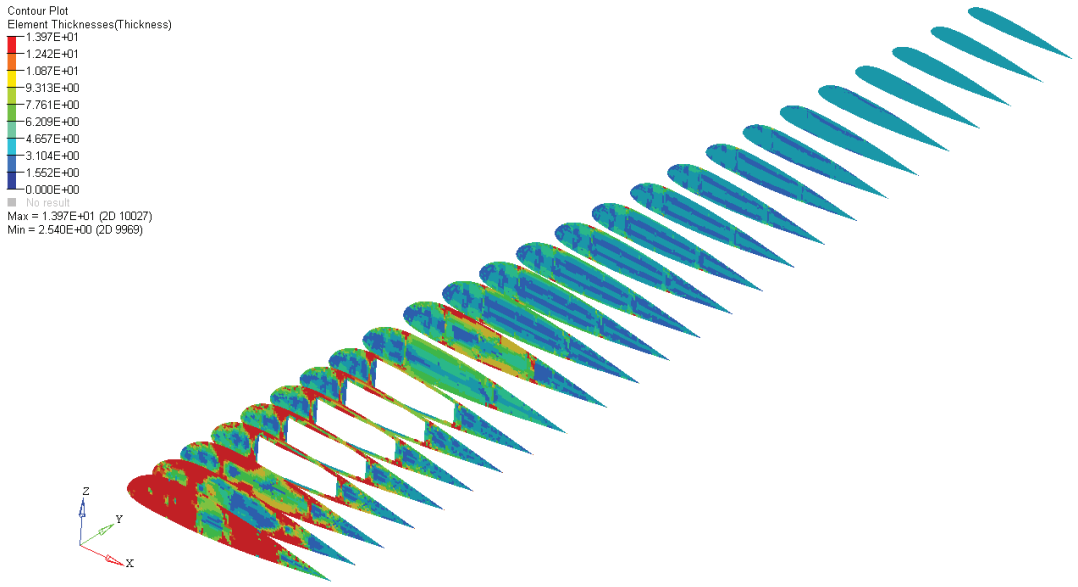

Fig. 14 Size Optimization Results of the Total ribs

Phase 3 – Detailed Design – Ply Stacking Sequence Optimization

The algorithm HyperShuffle is more aimed at providing a 'global view' of what the optimal stacking sequence could be. While shuffling the stacking sequence it is important that behavioral and design constraints are preserved. Further, it is required that certain ply book rules be applied to guide the stacking of plies based on specific requirements (not given here).

The ply bundle thus obtained is used for final laminate stacking. An algorithm HyperShuffle converts the dimensional ply bundle obtained above into local ply configuration or the final laminate. Fig. 15 shows the final laminate stacking sequence.

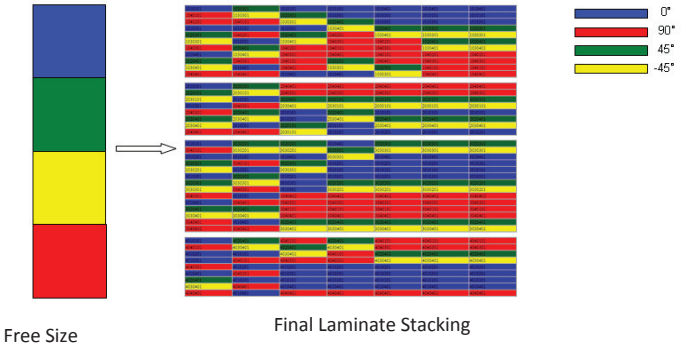

Fig 15 Final Laminate Stacking

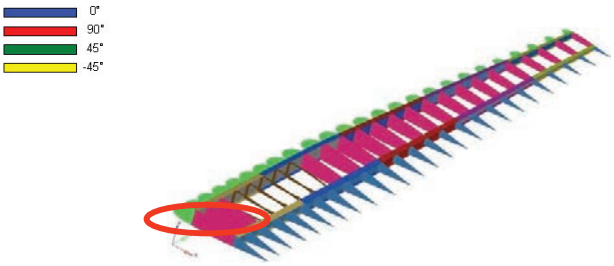

Fig. 16 Plies realized after shuffling the layers

The plies realized after shuffling the layers is given in Fig. 16. Optimized thickness for the patch on the rib marked is also given. Total ply thickness in the ribs varies from 2.54 to 13.97 mm. Similar optimization process is adopted for the skins and the Spars and not reported here.

5. Bird Hit on Composite Wing

Due to impact of a bird (or flock of birds) the wing is subjected to transient vibrations; the first step is to determine the lowest modes of vibration. The root of the composite wing in Fig. 16 is fixed in all degrees of freedom. For the wing in secton 4, Rao, Shvakumar (2015) determined the modes as given in Fig. 17 which also gives the bird model geometry approximated as a right circular cylinder with hemispherical end caps as shown.

An impact velocity of 125 m/s for the bird is given according to the FAA's Issue Paper G-1 that identifies the BA609 Certification Basis derived from applicable Parts 25 and 29 requirements of Title 14 Code of Federal Regulations (14 CFR). The time domain response is shown in Fig. 18 at five gauge point locations along with the frequency domain at the wing tip, gauge point 4.

Fig. 19 gives the FFT Output for Gauge Point #4. The Peaks marked correspond to the fundamental modes of vibration and this is in line with the Eigen Values and Eigen Vectors captured during the Modal Analysis Phase. The peaks corresponded to the first two chord-wise bending modes of the wing. These are the mode shapes which correspond to the impact mode.

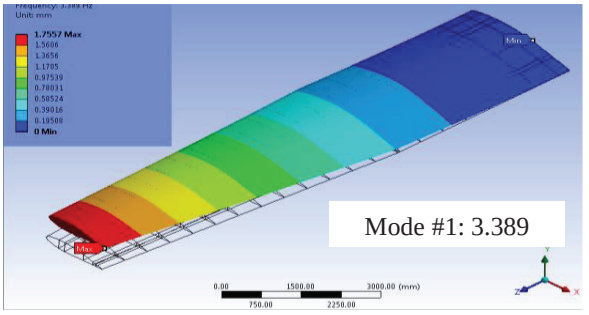

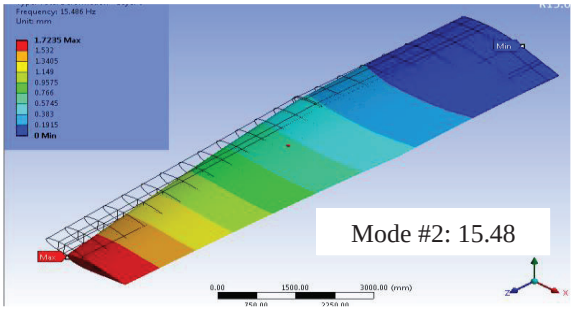

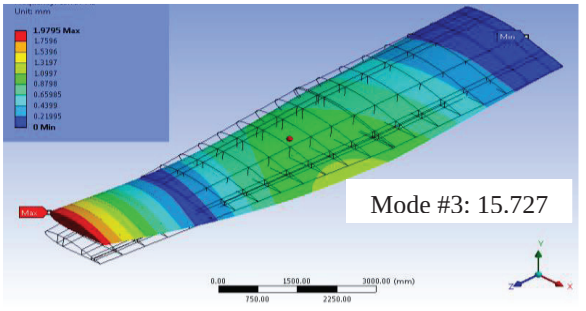

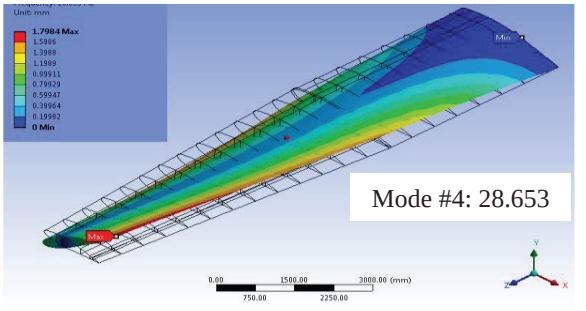

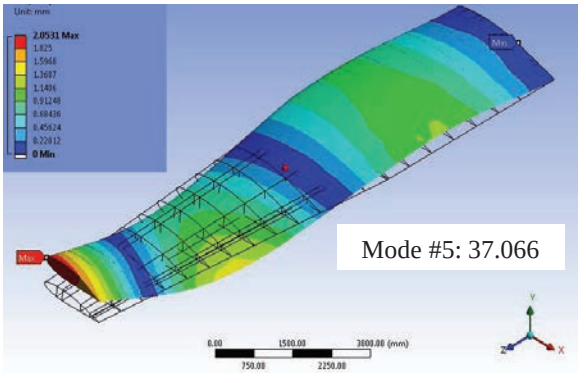

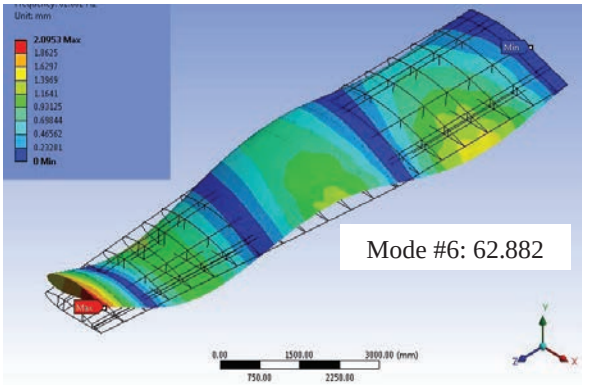

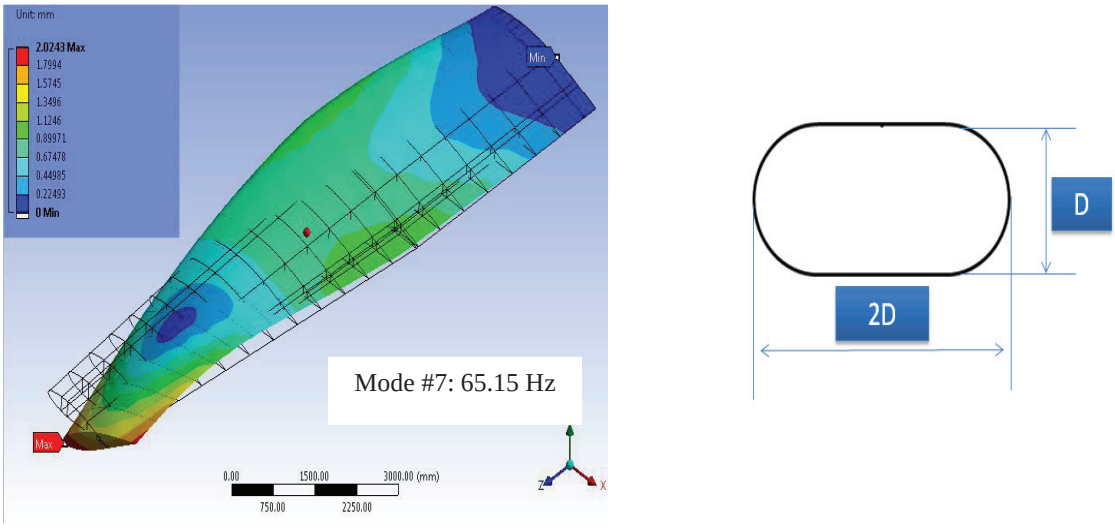

Fig. 17 First Seven Lower modes of vibration and the bird model

The problem thus formulated follows the understanding on impact and the results obtained are thus validated.

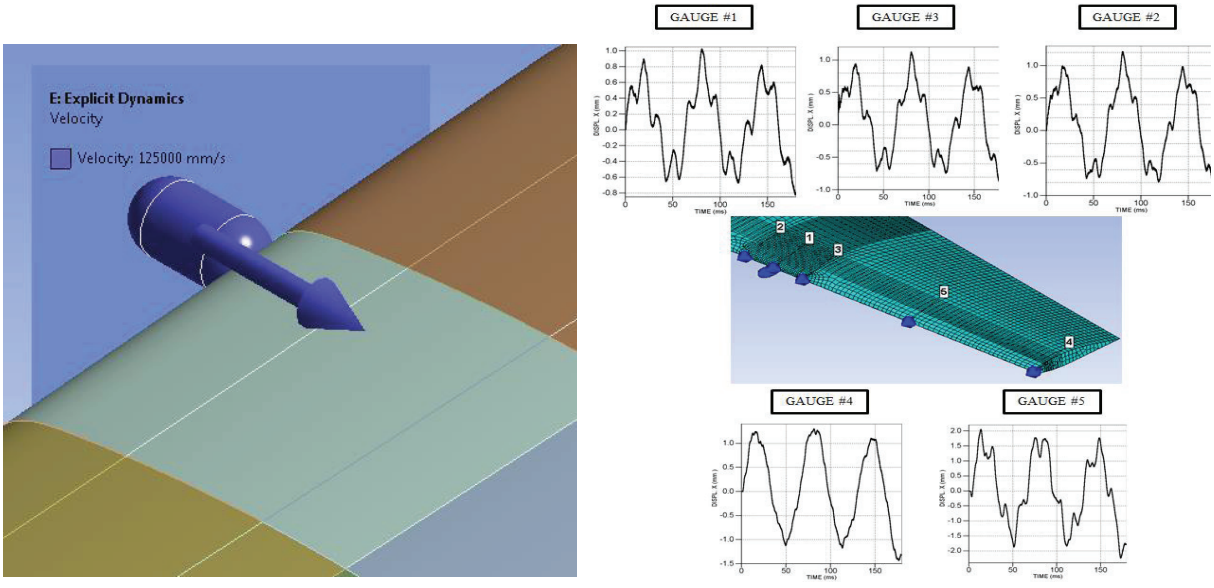

Fig. 18 Impact velocity applied as per FAA Bird Strike Conditions, time domain response at five gauge points

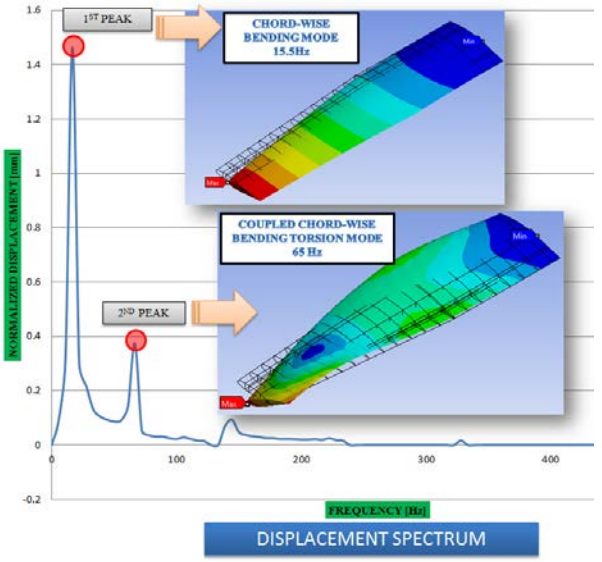

Fig. 19 FFT Output for Gauge Point #4

6. Fluid Structure Interaction and Flutter

Flutter is most commonly seen on wings and the control surfaces of an aircraft structure. It is because of the load acting on these are the highest when an aircraft is in flight. The inertia and flexibility of the structure plays a very significant role in the aeroelastic dynamic stability of the aircraft. Self-excited and unstable oscillations due to unsteady aerodynamic forces from the air flow normally take place when a structural system which is under flow conditions beyond some threshold or critical value of the flow parameter like the dynamic pressure. Flutter can be basically a phe-nomenon of unstable oscillations in a flexible structure. Further of the critical flow conditions for a structure, the occurrence of dynamic aeroelastic instability can be recognized by the exponential increase in the vibration amplitudes of the structural system with time. Aircraft structures including that of the rotating blades in a compressor that function as lifting surfaces are prone to flutter instability due to their interaction with the aerodynamic flow. The critical flow condition that leads to the onset of flutter is the 'Flutter Boundary' of the structure. The flutter boundary of an aerospace vehicle is a characteristic design parameter that is very important for practical design of its lifting surfaces. A cartoon depicting the perils of flutter is shown in Fig. 20. For a general introduction on flutter, reference may be made to Bisplinghoff and Ashley (1957).

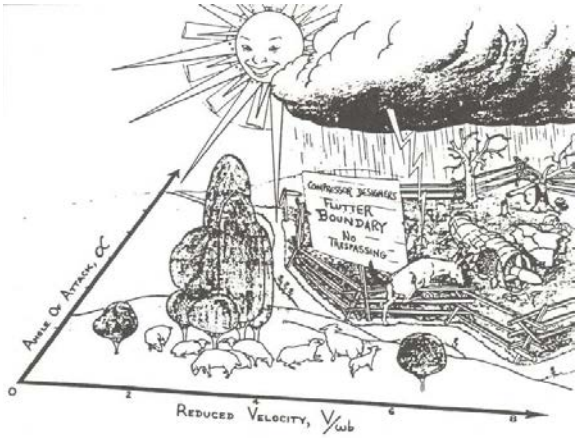

Fig 20 Cartoon depicting dangers of Flutter in a compressor

Classical methods gave way to CFD and Structural interaction in time domain. The 2D Flutter analysis of NACA 64_1 A212 with a two way coupled FSI model is illustrated in Fig. 21 with the structural and fluid domains, modal analysis results and pressure distribution over the wing surface, see Rao (2002).

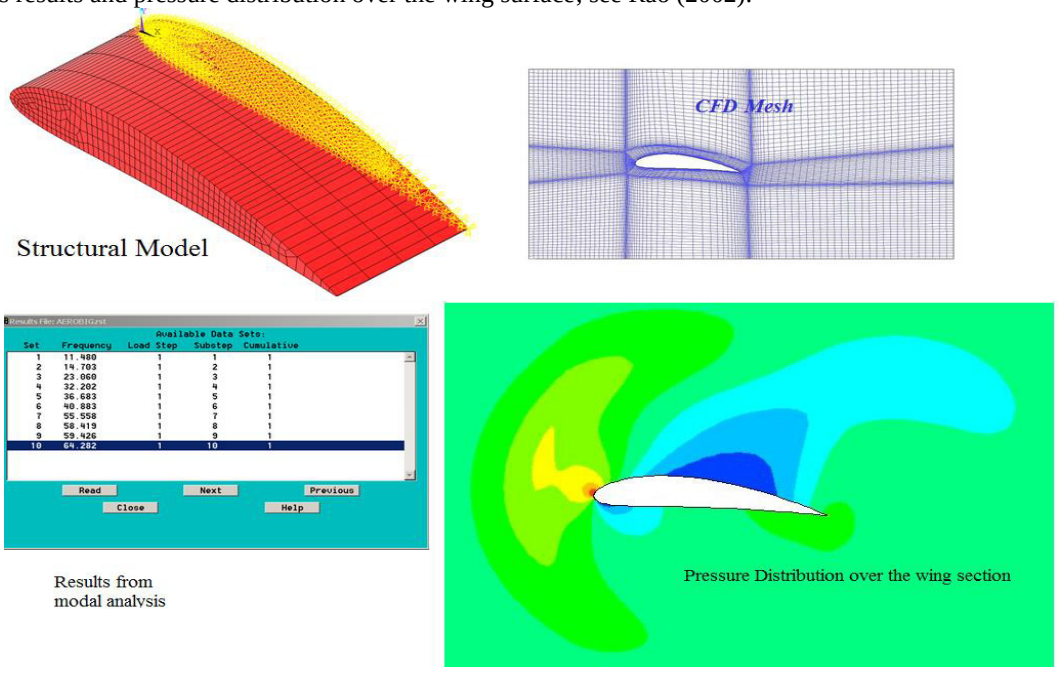

Fig 21 Aero elastic analysis of a NACA 64_1 A212 air foil

The vertical displacement obtained as a function of time for three velocities 100, 175 and 300 m/s loading conditions is given in Fig. 22. The flutter case can be seen here.

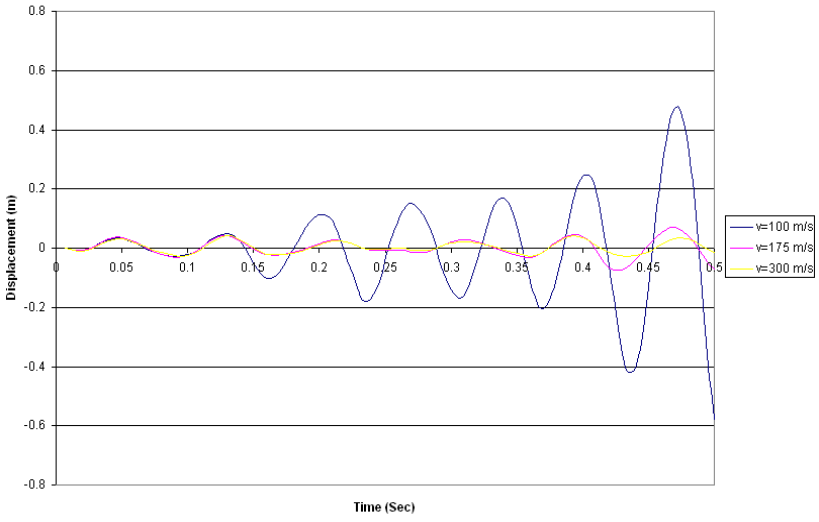

Fig 22 Vertical Displacement vs. Time Graph of the Air foil subjected to loading conditions

The computational cost of a coupled simulation with realistic models is quite high. We can utilize the historical data to constrain the aero elastic system to a certain step or point of simulation that it is solvable. Another way is to

design low order, high fidelity models which comprise most of the higher order, nonlinear effects. This kind of a system can give physical insight into the behaviour of the response problem.

6.1 3D Flutter Analysis

For the current study, the isotropic wing given in Fig. 9 is used. Figure 23 shows the mesh generated for the CFD analysis.

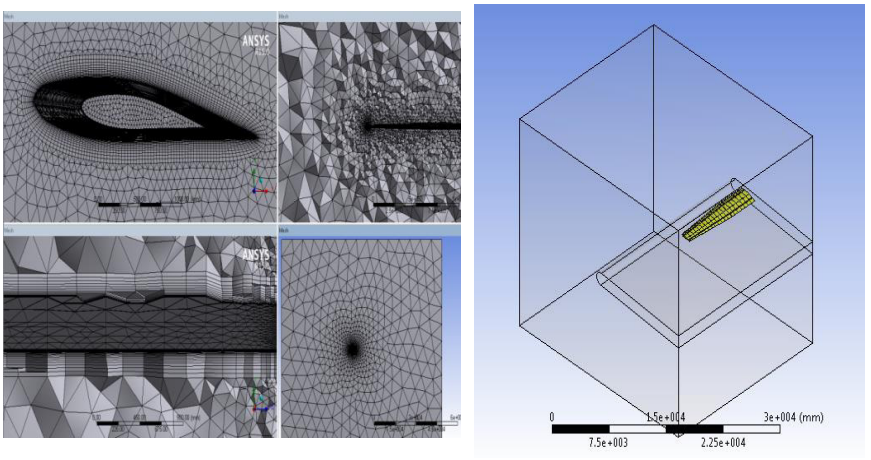

Fig 23 Computational Fluid Domain modelled for the analysis and the respective mesh.

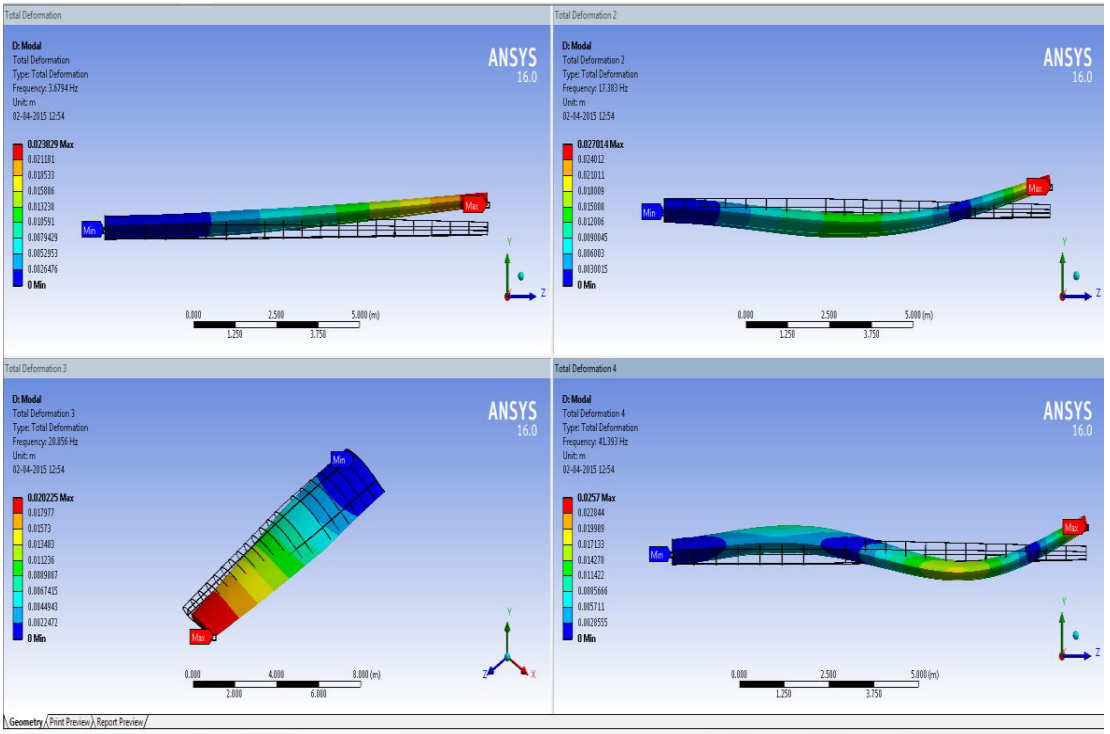

Fig 24 Modal Analysis

The total number of nodes generated are 104742 and the number of elements are 357048. More care was taken towards refinement of the mesh to capture the flow physics exactly and also to avoid negative volume error occuring due to the dynamic mesh in the analysis. The element quality parameters are: skewness: ~0.95 and orthogonality: ~0.02. In the analysis, Mach number is taken as 0.8 for three angles of attack, 0.05, 5 and 25 degrees.

The first four modes of vibration are given in Fig. 24, see Rao, Tharikaa and Shiva Kumar (2015). Three cases of angle of attack are considered.

Case 1: Angle of attack 0.05^0

The dynamic FSI analysis was carried out for 0.5 s with a time step of 0.001 s. Fig. 25 gives the fluid velocity at the wing tip at 0.5 s. Similarly the fluid pressure at the wing tip is given in Fig. 26. Transient response at the wing tip is given in Fig 27. This clearly shows that the response is decaying without causing any flutter conditions.

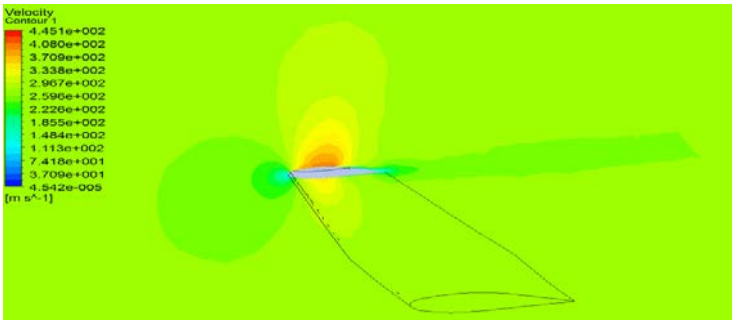

Fig 25 Contours of fluid velocity at the wing tip at 0.5 s for angle of attack 0.05 degrees

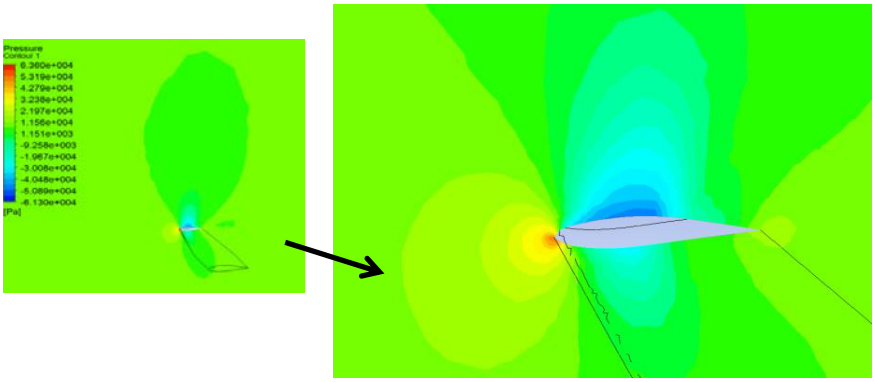

Fig 26 Contours of fluid pressure at the wing tip at 0.5 s for angle of attack 0.05 degrees

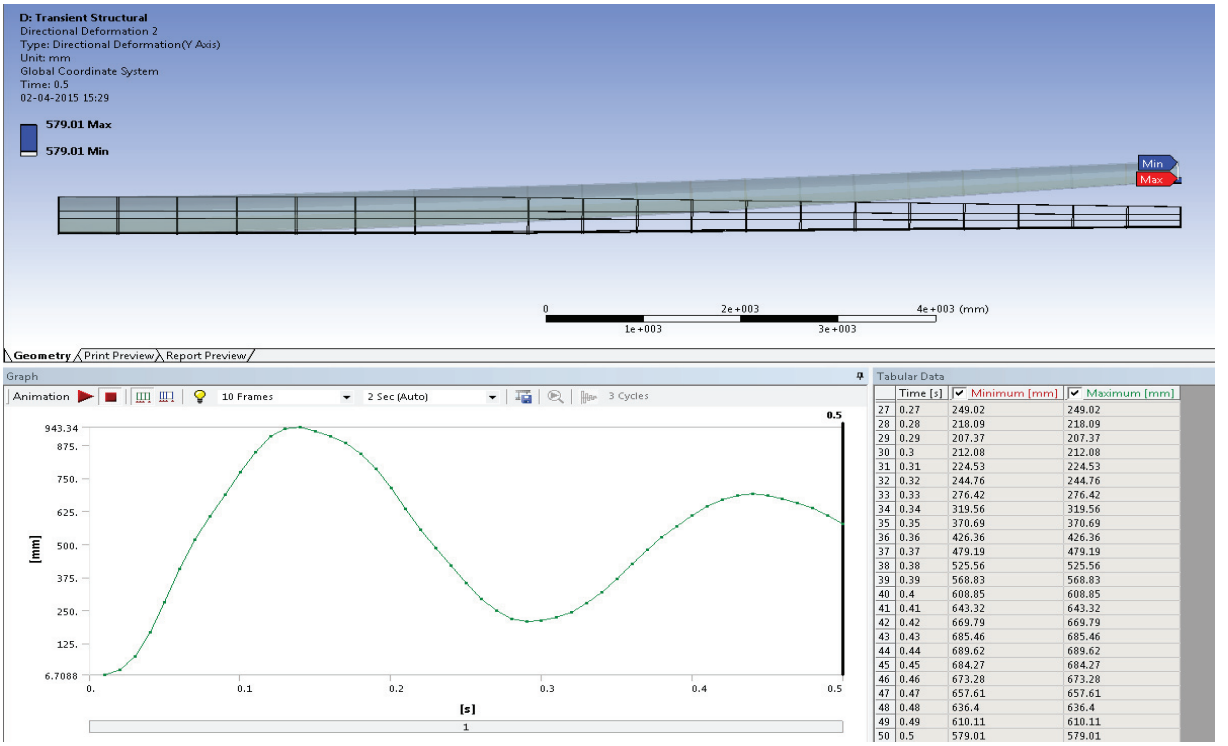

Fig 27 Time Response curve of the wing tip for first bending mode

Figure 28 shows the frequency response of the time domain signal. Only one peak is present corresponding to I mode 3.67 Hz.

Case 2: Angle of attack 5^0

The dynamic FSI analysis was carried out for 0.81 s at 5^0 with a time step of 0.001 s. Fig. 29 gives the fluid pressure at the wing tip at 0.81 s.

Similarly the fluid velocity at the wing tip is given in Fig. 30.

In Fig 31 Pressure applied on wing exerted by the fluid is compared at the initial and final time steps as the peak pressure rose to the nose region.

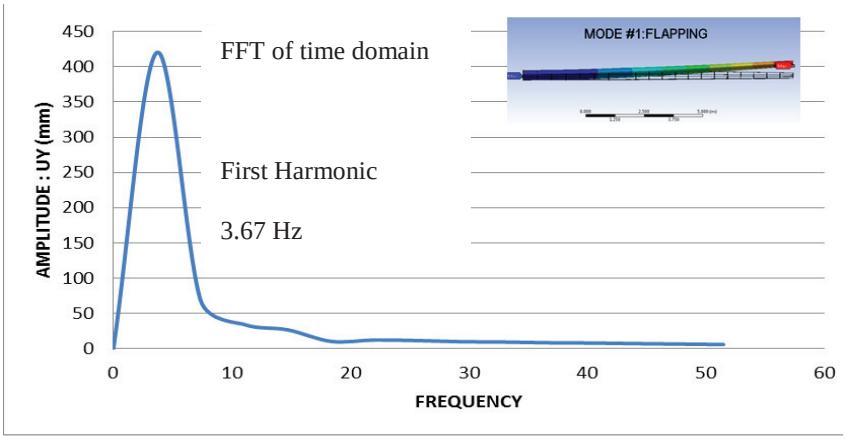

Fig 28 Frequency Response of case 1

In Fig. 32 the wing displacemt is shown at the first and last time steps showing prevailing flutter conditions.

The flow streamlines at the initial time step indicates steady conditions, whereas at the last time step, the streamlines are not steady as shown in Fig. 33. The response of the wing tip upto 0.81 s is given in Fig. 34 showing the flutter condition.

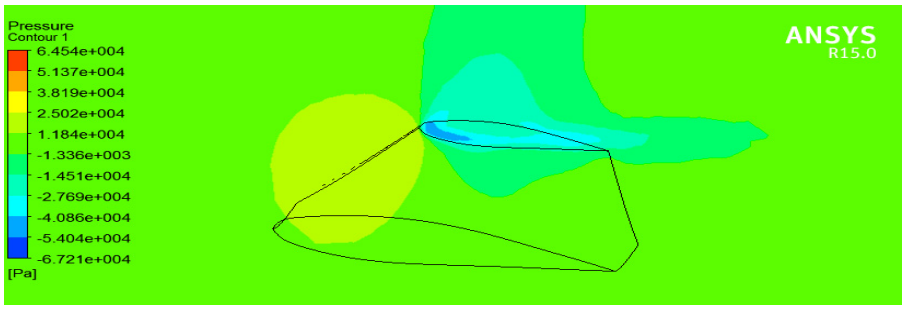

Fig 29 Contours of Pressure at the wing tip at 0.81 s for angle of attack 5 degree

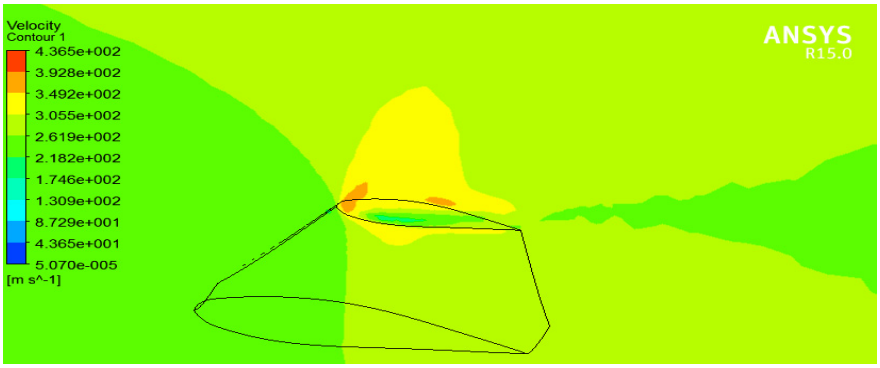

Fig 30 Contours of Velocity at the wing at 0.81 s for angle of attack 5 degree

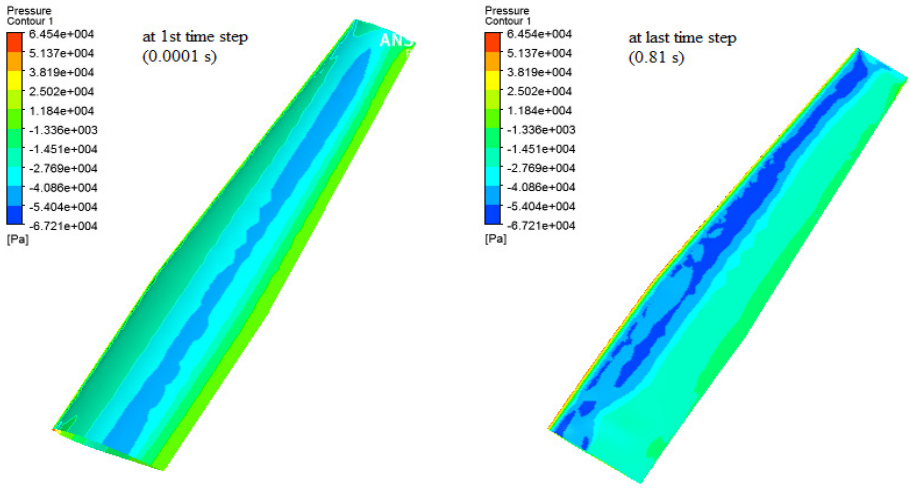

Fig 31 Comparison of Pressure applied on wing exerted by the fluid for angle of attack 5 degree

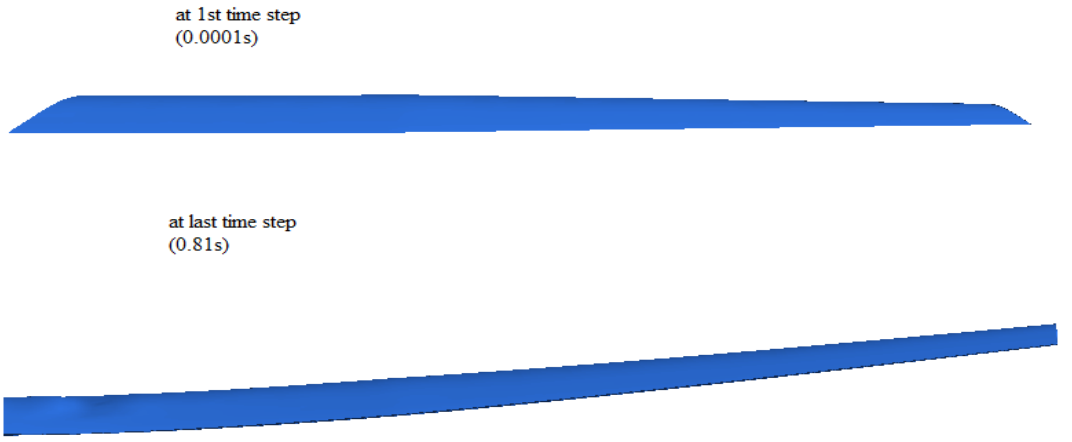

Fig 32 Wing deformation at the first and last time steps

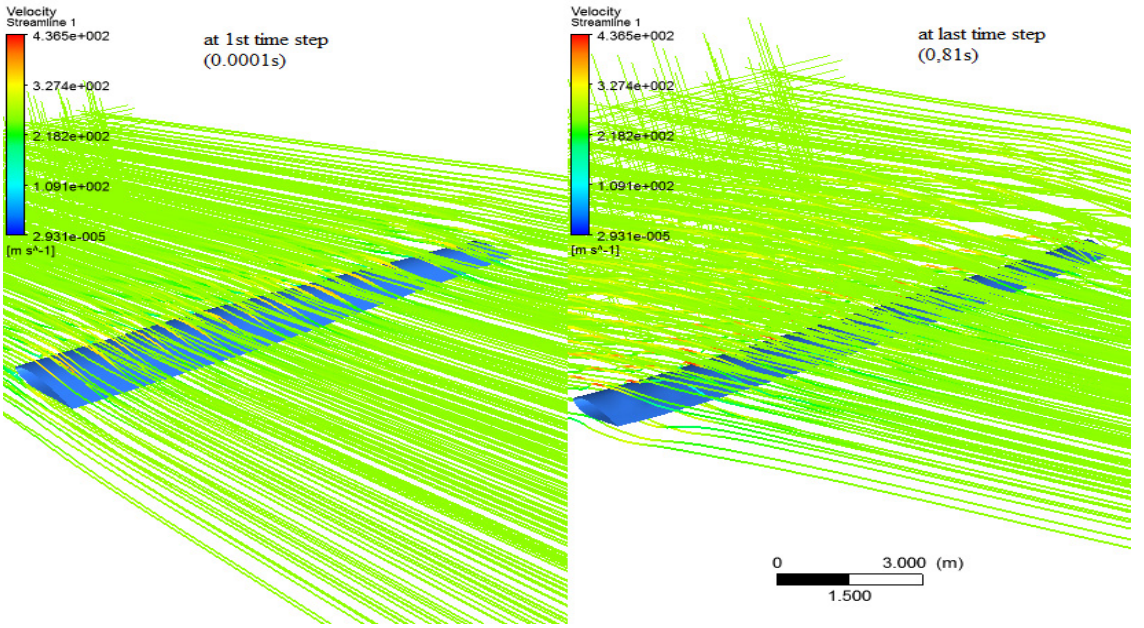

Fig 33 streamlines of velocity over the wing at the first and last time step at 0.81 s

Case 3: Angle of attack 25^0

By increasing the angle of attack further the flutter is expected to be severe. In this case the response increased rapidly and the numerical instability terminated the run at 0.327 s. The dynamic Figs. 35 and 36 give the fluid pressure and velocity at the wing tip at 0.327 s respectively. Fig 37 gives the vibration amplitude at the wing tip which shows no oscillation.

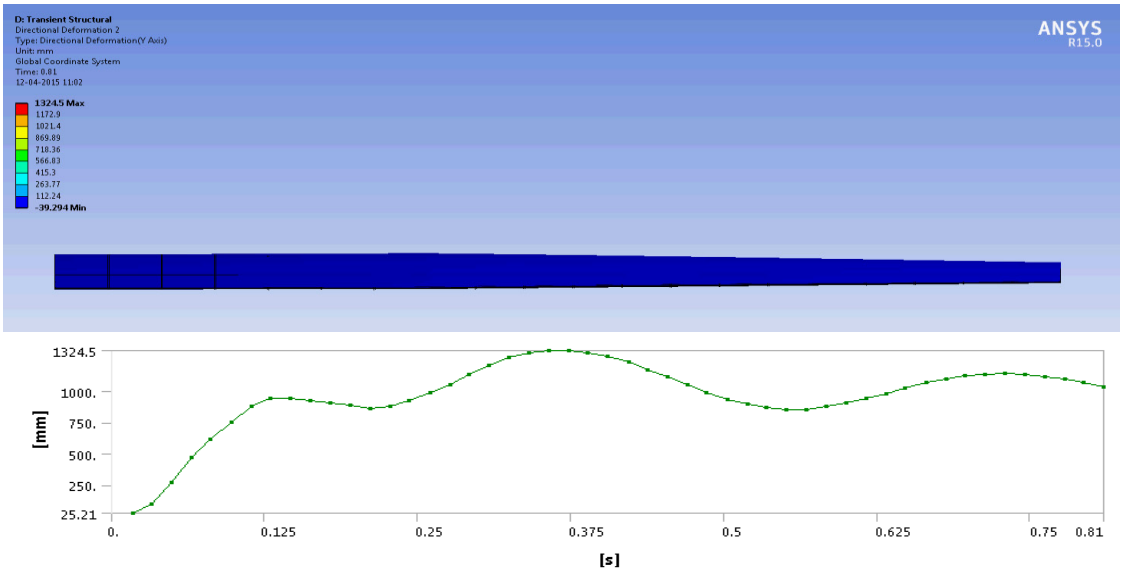

Fig 34 Time Response curve of the wing tip upto 0.81 s for angle of attack 5 degree

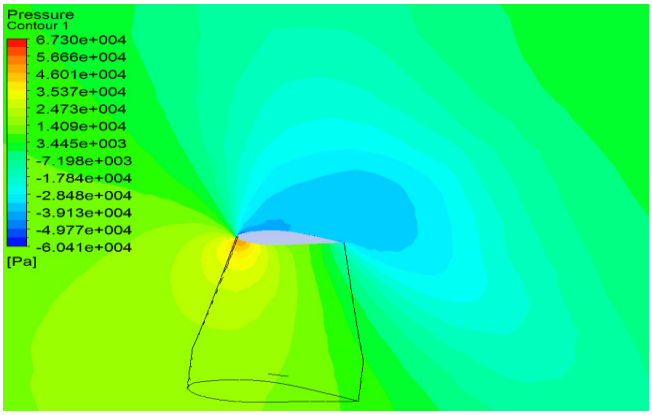

Fig 35 Contours of pressure at the wing tip at 0.327 s for angle of attack 25 degree

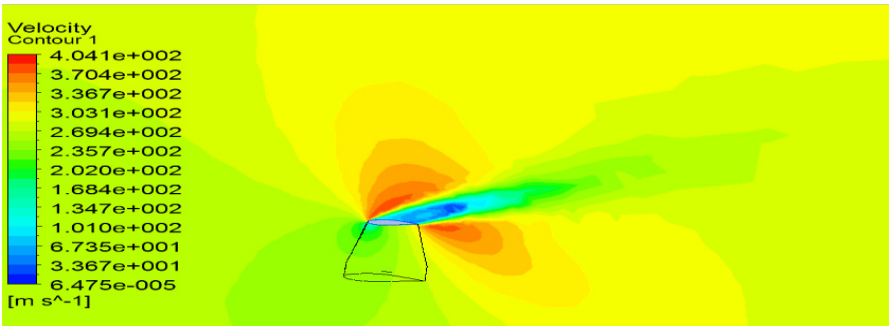

Fig 36 Contours of velocity of fluid at the wing tip at 0.327 s for angle of attack 25 degree

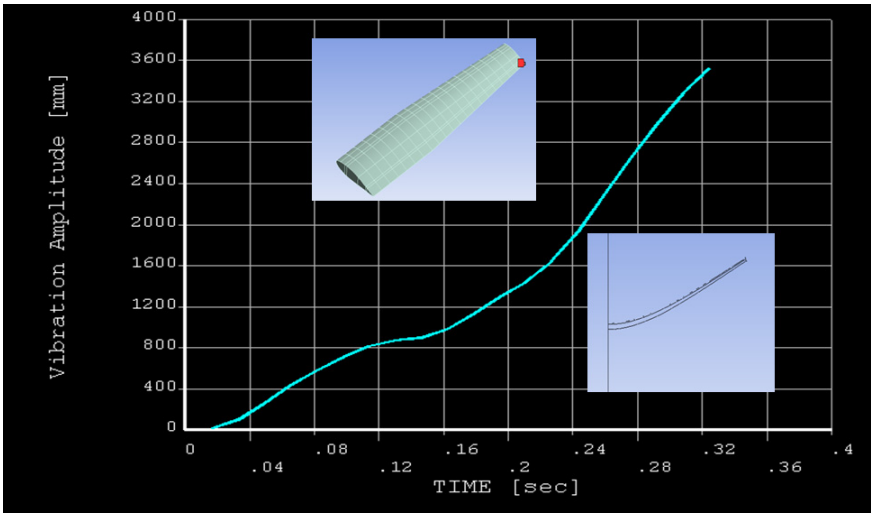

Fig 37 Response of the wing tip

7. Coupled Large Scale Problems in Aero Structures

Aircraft structures are some of the challenging problems with huge number of elements both solid and fluid. The structure has very low frequencies that participate in dynamics and fluid structure interaction. The problem becomes more complex when the Engine mounted on the Wing is accounted for with several rotating stages of turbine and compressor on a flexible drum like shafting with two or three spools. Then the problem is much more challenging when fluid structure interaction of the wing, engine and its rotating parts and gets further complicated if we are looking at time domain analysis, particularly flutter of the aircraft and rotating stages.

Assuming that the fuselage is relatively rigid, the wing plays a significant role and the computational time in time domain becomes unwieldy. Fig. 38 shows such a complex model.

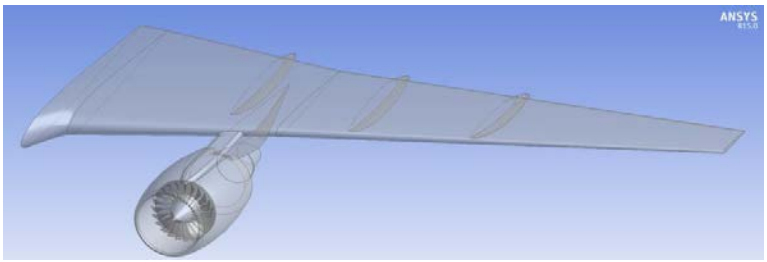

Fig 38 Wing and Engine Model

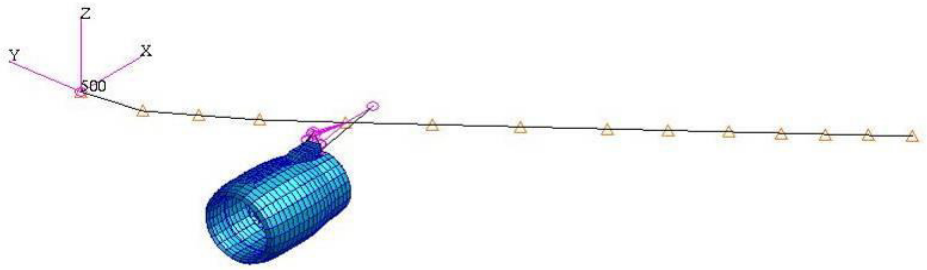

Fig 39 Wing and Engine Super Element Model

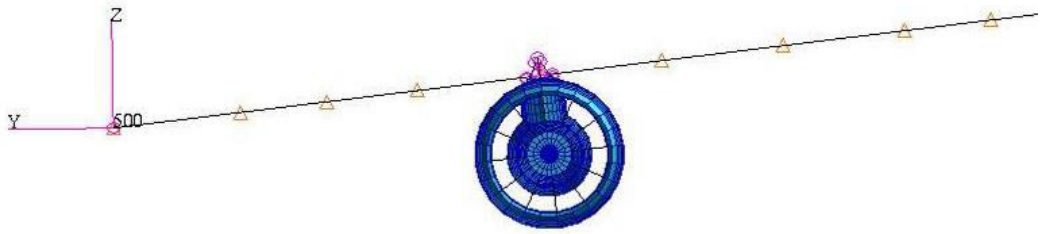

Fig 40 Wing and Engine Super Element Model

8. Bird Flock Impact

On January 15, 2009, US Airways Flight 1549 from LaGuardia Airport to Charlotte/Douglas Airport had to be ditched in the Hudson River after being disabled by striking a flock of Canada geese during its initial climb out, see Fig. 41. This event has shown the necessity of estimating crack propagation life due to severe nonsteady pressure field from the bird strike.

Fig. 41 US Airways Flight encountering Canadian Geese

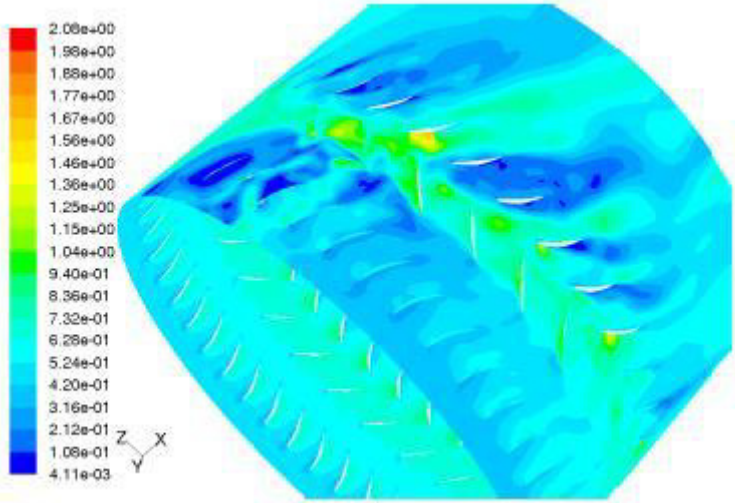

Fig. 42 Shock Flow in the Blocked Area

The conventional practice of treating a foreign object ingestion into a gas turbine engine is to treat the problem as one of an Eulerian modeled particles (or Solid Particle Hydrodynamics model) impacting a Lagrangian modeled structure. While this analysis allows the determination of structural integrity it fails in estimating flow interference between the stator and rotor stages and determining the resonant response leading to life estimation of the blades. Here the transient pressure field on the rotor blade due to sudden blockage of the passages from a flock of birds is considered to estimate the dynamic pressure field that causes the alternating stress field on the rotor blades for fracture analysis. Rao and Rzadkowski (2014) considered this problem and estimated crack propagation life by considering the engine flow path alone.

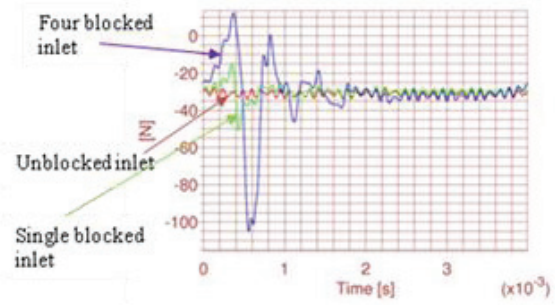

Fig. 43 Resulting shock load nearly 100 times the nominal nozzle passing load

Due to this severe shock loading it was calculated that a crack induced will take just 7 sec for failure resulting in a sudden blade-off condition. The structural integrity of the engine and the aircraft structure as a whole is in jeopardy. The super-element model in Figs. 39 and 40 can be helpful in making this estimate of life.

Acknowledgements

The author is deeply indebted to late Arutselvar Padmabhushan Dr. Mahalingam for his mentorship and encouragement in carrying out advanced design projects and cultivating the spirit of bringing Science Revolution benefits to Engineering through High Performance Computing.

References

[1] Altair HyperWorks (2011)
[2] Bendsøe MP and Kikuchi N (1988) Generating optimal topologies in optimal design using a homogenization method. Comp. Meth. Appl. Mech. Eng. 71, p. 197.
[3] Bendsøe MP and Sigmund O (2003) Topology Optimization–Theory, Methods and Applications, Springer Verlag, Berlin/Heidelberg
[4] Bendsøe MP et al., (1994) An Analytical Method to Predict Optimal Material Properties in the Context of Optimal Structural Design, J of Applied Mechanics, vol. 61, No. 4, p. 930
[5] Bendsøe MP et al., (1995) Optimal Design of Material Properties and Material Distribution for Multiple Loading Conditions, Intl J for Numerical Methods in Engineering., vol. 38, No. 7, p. 1149
[6] Bisplinghoff, RL and Ashley H, (1957) Aero elasticity; Addison- Wesley Publication
[7] Crombie AC (1979) Augustine to Galileo, Harvard University Press
[8] Heath TL (1897) The works of Archimedes, ed. in modern notation, with introductory chapters, Cambridge: University press
[9] Heath TL (1921) A History of Greek Mathematics, Oxford
[10] Heath TL (1956) The Thirteen Books of Euclid's Elements, translation and commentaries in three volumes. Dover
[11] Keng-Tuno C (1981) On Non-smoothness in Optimal Design of Solid, Elastic Plates, International Journal of Structures, vol. 17, No. 8, p. 795
[12] Pederson O (1993) Early Physics and Astronomy: A Historical Introduction, 2nd. ed., Cambridge University Press
[13] Pike RW (1992) Optimization for Engineering Systems, Louisiana State University
[14] Rao JS (1992) Advanced Theory of Vibrations, John Wiley & Sons

[15] Rao, JS (1998) Dynamics of Plates, Narosa, Marcel Dekker and Alpha Science
[16] Rao, JS (2002) Recent advances in India for airframe & aero engine design and scope for global cooperation, AECMA-SIATI, Aero Technologies Summit, November 26-28, 2002, Bangalore.
[17] Rao JS (2003), Recent Advanced in India for Airframe & Aero engine Design and Scope for Global Cooperation, Society of Indian Aerospace Technologies & Industries, 11th Anniversary Seminar, February 8, 2003, Bangalore
[18] Rao JS (2011) History of Rotating Machinery Dynamics, Springer
[19] Rao, JS (2012) Optimization and Analysis Unified, 57th Congress of Indian Society of Theoretical and Applied Mechanics, 16-18 December 2012, Pune
[20] Rao JS, Kiran S, Chandra S, Kamesh JV and Padmanabham MA (2008) Concept Design of Aircraft Wing, (Topology Optimization approach), Aerotech 2008 National Seminar on “Recent Advances in Aerospace Technologies, Maintenance & Optimization”, Bangalore
[21] Rao JS, Saravanakumar M and Sunil Kumar (2006) Flow Optimization with Conjugate Heat Transfer, G.I. Taylor Memorial Lecture, Proceedings 51st Annual Congress Indian Society of Theoretical and Applied Mechanics, December 18 - 20, Visakhapatnam, India
[22] Rao JS and Kiran S (2010) Concept Design of Composite Aircraft Wing, Proceedings of the ASME 2010 International Mechanical Engineering Congress & Exposition, IMECE2010-37206, November 12-18, 2010, Vancouver, British Columbia, Canada
[23] Rao JS and Rzadkowski R (2014) Crack Propagation Life Calculation of an Aircraft Compressor Blade due to Bird Injestion, GT2014-25010, Proceedings of the ASME Turbo Expo 2014, June 16-20, Dusseldorf, Germany
[24] Rao JS and Shiva Kumar P (2015) Bird Strike Analysis Composite Wing GT2015-42818, Proceedings of the ASME Turbo Expo 2015: Turbine Technical Conference and Exposition, June 15-19, 2015, Montréal, Canada
[25] Rao JS and Suresh S (2006) Blade Root Shape Optimization, The Future of Gas Turbine Technology, 3rd International Conference, 11-12 October, Brussels, Belgium, Paper ST T2-3
[26] Rao JS, Tharikaa RK and Shiva Kumar P (2015) Flutter of an Aircraft Wing, ICVE, Shanghai
[27] Rickey VF (1996) Brachistochrone, Historical Notes for the Calculus Classroom, http://www.math.usma.edu/people/rickey/hm/CalcNotes/brachistochrone.pdf
[28] Timoshenko SP (1960) Strength of Materials, D Van Nostrand Company
[29] Vanderplaats GN (1984) Numerical Optimization Techniques for Engineering Design with Applications, McGraw-Hill.